

Valproic acid inhibits A β production, neuritic plaque formation, and behavioral deficits in Alzheimer's disease mouse models

Hong Qing,¹ Guiqiong He,^{1,3} Philip T. T. Ly,^{1,2} Christopher J. Fox,^{1,2} Matthias Staufenbiel,⁴ Fang Cai,¹ Zhuohua Zhang,⁵ Shengcai Wei,¹ Xiulian Sun,^{1,2} Chia-Hsiung Chen,^{1,2} Weihui Zhou,¹ Ke Wang,^{1,2} and Weihong Song^{1,2}

¹Townsend Family Laboratories, Department of Psychiatry, Brain Research Center, ²Graduate Program in Neuroscience, University of British Columbia, Vancouver, BC V6T 1Z3, Canada

³Department of Human Anatomy, Chongqing University of Medical Sciences, Chongqing 400016, China

⁴Novartis Institutes for Biomedical Research Basel, CH-4002 Basel, Switzerland

⁵Center for Neuroscience and Aging, The Burnham Institute, La Jolla, CA 92037

Neuritic plaques in the brains are one of the pathological hallmarks of Alzheimer's disease (AD). Amyloid β -protein (A β), the central component of neuritic plaques, is derived from β -amyloid precursor protein (APP) after β - and γ -secretase cleavage. The molecular mechanism underlying the pathogenesis of AD is not yet well defined, and there has been no effective treatment for AD. Valproic acid (VPA) is one of the most widely used anticonvulsant and mood-stabilizing agents for treating epilepsy and bipolar disorder. We found that VPA decreased A β production by inhibiting GSK-3 β -mediated γ -secretase cleavage of APP both in vitro and in vivo. VPA treatment significantly reduced neuritic plaque formation and improved memory deficits in transgenic AD model mice. We also found that early application of VPA was important for alleviating memory deficits of AD model mice. Our study suggests that VPA may be beneficial in the prevention and treatment of AD.

CORRESPONDENCE

Weihong Song:
weihong@interchange.ubc.ca

Abbreviations used: A β , amyloid β -protein; AD, Alzheimer's disease; APP, β -amyloid precursor protein; BACE, β -site APP cleaving enzyme; CTF, C-terminal fragment; GSK, glycogen synthase kinase; HDAC, histone deacetylase; MAP, microtubule-associated protein; VPA, valproic acid.

Alzheimer's disease (AD) is the most common neurodegenerative disorder leading to dementia. Neuritic plaques, neurofibrillary tangles, and neuronal loss represent the main histological hallmarks observed in AD brains. Amyloid β -protein (A β), the central component of senile plaques, is produced from sequential endoproteolytic cleavages of the type 1 transmembrane glycoprotein β -amyloid precursor protein (APP) by β - and γ -secretase (1). β -Site APP cleaving enzyme 1 (BACE1) is the β -secretase in vivo (2–6). γ -Secretase is an atypical multimeric membrane-protein aspartic protease composed of at least four subunits: presenilin (PS1 or PS2), nicastrin (Nct), APH-1 (APH-1aL, APH-1aS, or APH-1b), and PEN-2 (7–11). More recently, two additional proteins, CD147 and TMP21, were found to be closely associated with the γ -secretase complex (12, 13). The components of the γ -secretase complex are tightly regulated

with each other, and PS1 is generally believed to be its catalytic core (14, 15). Another important substrate of γ -secretase is Notch, whose intracellular domain (NICD) is released upon γ -secretase cleavage and translocates to the nucleus, where it can activate transcription of downstream target genes (8, 10). In addition to its role in Notch signaling and APP processing, γ -secretase is also involved in regulating intramembraneous proteolysis of many other type I integral membrane proteins, such as Jagged, Delta, E-cadherin, ErbB-4, Nectin-1 α , CD44, and LRP (16–22). Missense mutations in the PS1 and PS2 genes are major causes of early-onset familial AD (23–25). Although the underlying mechanism of AD neurodegeneration is currently unclear, A β accumulation appears to play a critical role in AD pathogenesis.

H. Qing, G. He, and P.T.T. Ly contributed equally to this paper. The online version of this article contains supplemental material.

© 2008 Qing et al. This article is distributed under the terms of an Attribution–Noncommercial–Share Alike–No Mirror Sites license for the first six months after the publication date (see <http://www.jem.org/misc/terms.shtml>). After six months it is available under a Creative Commons License (Attribution–Noncommercial–Share Alike 3.0 Unported license, as described at <http://creativecommons.org/licenses/by-nc-sa/3.0/>).

Valproic acid (VPA) is one of four first-line antiepileptic drugs being increasingly used in the treatment of bipolar disorder. Like other anticonvulsants, VPA inhibits sodium, potassium, and calcium channel functions. Although its direct *in vivo* target has yet to be definitively identified (26), VPA may enhance γ -aminobutyric acid transmission (27). VPA has been found to activate extracellular signal-regulated kinase, a protein kinase known to regulate AP-1 function, and mediate neurotrophic responses (28). VPA treatment could lead to a change in glycogen synthase kinase (GSK-3) and histone deacetylase (HDAC) activity (29). Furthermore, VPA, like lithium, regulates the Wnt signaling pathway by increasing β -catenin expression (30). Increased β -catenin expression is also seen after treatment with the chemically unrelated HDAC inhibitor trichostatin A. This mechanism may explain some effects of VPA on gene expression and neurodevelopment (31). It has been shown that increased histone acetylation by HDAC inhibitors facilitates synaptogenesis and improves learning and memory, suggesting that inhibition of HDAC may be a suitable therapeutic avenue for neurodegenerative diseases (32).

In this study, we examined the effects of VPA on AD neuropathology and behavioral deficits and identified its underlying mechanism. We found that VPA inhibited GSK-3 β -mediated γ -secretase cleavage of APP both *in vitro* and *in vivo*. Furthermore, such inhibition decreased A β production and neuritic plaque formation, as well as alleviated the memory deficits in AD transgenic model mice. Our data suggest that VPA is effective for anti-amyloid therapy in the prevention and treatment of AD.

RESULTS

VPA inhibits A β deposition and neuritic plaque formation in AD transgenic mice

To assess the effect of VPA treatment on AD neuropathology, APP23 transgenic mice, which are an AD mouse model, were subjected to VPA treatment. APP23 mice carry the human Swedish mutant APP751 transgene driven by the neuronal-specific Thy1.2 promoter (Fig. S1, available at <http://www.jem.org/cgi/content/full/jem.20081588/DC1>). APP23 mice develop amyloid plaques in the neocortex and hippocampus as early as 6 mo (33). APP23 mice were treated with 30 mg/kg VPA at 7 mo of age, whereas age-matched control APP23 mice received vehicle solution. To investigate whether VPA treatment could result in neuropathological changes *in vivo*, VPA-treated and control mice were killed after treatment and behavioral tests. 4G8 immunostaining and thioflavin S staining were used to detect A β -containing neuritic plaques in the brain (Fig. 1, A and B). Neuritic plaque formation was significantly decreased in APP23 mice treated with VPA (Fig. 1 A, b), relative to controls (Fig. 1 A, a). Quantification showed that overall VPA treatment reduced plaque number by ~4-fold (3.5 ± 0.79 vs. 14.95 ± 2.09 per slice; $P < 0.0001$; Fig. 1 D). The effects were similar among mice killed either immediately, 1 mo, or 2 mo after treatment and behavioral testing (0.75 ± 0.48 vs. 5.50 ± 1.32 , $P < 0.001$; 2.33 ± 0.50 vs. 10.33 ± 1.26 , $P < 0.001$; and 5.30 ± 1.33 vs. 21.5 ± 02.76 ,

$P < 0.001$, respectively; Fig. S2). APP23 mice were also treated with VPA at 9 mo of age. Significantly more neuritic plaques were formed in the mice at 9 mo compared with 7 mo of age; however, VPA treatment starting at the age of 9 mo could also significantly reduce neuritic plaque formation (Fig. 1 A, c and d). The number of plaques in VPA-treated and control mice were 11.09 ± 0.92 and 25.60 ± 3.50 , respectively ($P < 0.005$; Fig. 1 E). The area of plaques was also significantly reduced in VPA-treated mice compared with control by 43.10 \pm 11.13% for the 7-mo-old group ($P < 0.01$) and by 59.66 \pm 5.44% for the 9-mo-old group ($P < 0.05$). In addition to reducing neuritic plaque formation, VPA treatment also significantly increased microtubule-associated protein (MAP)-2 immunoreactivity (Fig. 1 C), which indicated a protective effect on dendritic damages and promoting neurite outgrowth in the transgenic mice. Similar results were obtained with silver staining (unpublished data).

To further confirm VPA's effect on AD pathogenesis, APP23 transgenic mice were crossbred with PS45 transgenic mice to generate APP23/PS45 double-transgenic mice. PS45 mice have an overexpression of the human familial AD-associated G384A mutant presenilin-1. The double-transgenic mice developed detectable neuritic plaques in the neocortex and hippocampus as early as 1 mo of age. Double-transgenic mice were treated with 30 mg/kg VPA at 6 wk of age for 4 wk. VPA treatment markedly inhibited neuritic plaque formation (Fig. 1 A, f and d) and significantly reduced plaque numbers from 14.84 ± 1.67 to 2.862 ± 0.65 ($P < 0.0001$; Fig. 1 F). Thioflavin S staining also confirmed VPA-induced reduction of A β -containing neuritic plaque formation in the brains of APP23 single-transgenic (Fig. 1 B, b and a) and APP23/PS45 double-transgenic (Fig. 1 B, d and c) mice. Over the 4-wk injection period, VPA treatment did not affect food and water consumption of the mice, and no significant weight changes were observed between the treatment and control groups (unpublished data). These data clearly demonstrate that VPA inhibits A β neuritic plaque formation *in vivo*.

VPA treatment significantly improves memory deficits in AD model mice

To investigate whether VPA treatment affects learning and memory in AD pathogenesis, behavioral tests were performed after APP23 mice received 1 mo of VPA treatment starting at the age of 7 mo. The Morris water maze was used to determine the effect of VPA on spatial memory. In the visible platform tests, VPA-treated and control APP23 mice had similar escape latency (53.190 ± 1.56 and 49.75 ± 2.47 s; $P > 0.05$; Fig. 2 A) and path length (7.03 ± 1.33 and 6.78 ± 1.60 s; $P > 0.05$; Fig. 2 B), which indicated that VPA treatment did not affect mouse motility or vision. In the hidden platform-swimming test, APP23 mice treated with VPA showed significant improvements compared with the vehicle-treated controls. The escape latency on the third and fourth day of the hidden platform test was shorter (15.95 ± 1.61 and 12.80 ± 1.83 s) than nontreated APP23 mice (29.04 ± 2.99 and 24.89 ± 3.33 s; $P < 0.001$; Fig. 3 C). The VPA-treated mice were able to

swim significantly shorter distances to reach the platform (3.88 ± 0.91 and 2.68 ± 1.02 m) compared with control mice (6.03 ± 0.94 and 5.37 ± 1.38 m) on the third and fourth day ($P <$

0.01 ; Fig. 2 D). In the probe trial on the last day of testing, the platform was removed. VPA treatment significantly improved the AD mouse's spatial memory. The number of times the

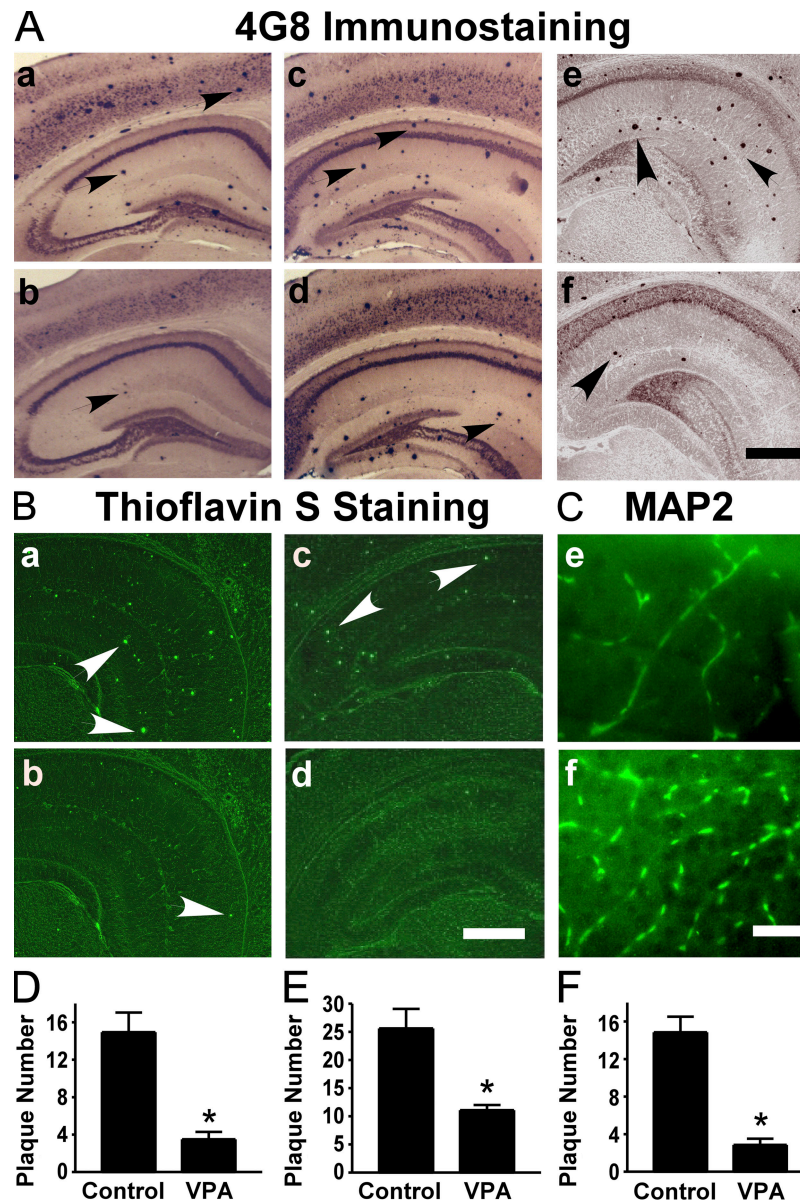


Figure 1. VPA treatment significantly reduces neuritic plaque formation in AD transgenic mice. (A) APP23 mice at the age of 7 or 9 mo and APP23/PS45 double-transgenic mice at the age of 6 wk were treated with 30 mg/kg VPA for 4 wk, whereas age-matched control APP23 mice received the vehicle solution. The mice were killed after behavioral tests and the brains were dissected, fixed, and sectioned. Neuritic plaques were detected using an A β -specific monoclonal antibody 4G8 and the DAB method. The plaques were visualized by microscopy with 40X magnification. The number of neuritic plaques was significantly reduced in VPA-treated mice compared with controls. b, d, and f show the representative brain section of the 7-mo APP23 age group, 9-mo APP23 age group, and APP23/PS45 mice treated with VPA, and a, c, and e show their controls, respectively. Black arrows point to plaques. (B) Neuritic plaques were further confirmed using thioflavin S fluorescent staining and visualized by microscopy at 40X magnification. There were less neuritic plaques in VPA-treated mice (b and d) compared with age-matched control mice (a and c). a and b show brain sections of APP23 mice, and c and d show the brain sections of APP23/PS45 mice. White arrows point to green fluorescent neuritic plaques. (C) The brain sections of APP23 were also stained with MAP-2 antibody. VPA treatment significantly increased the number of MAP-2-positive neurites. Bars: (A and B) 400 μ m; (C) 200 μ m. (D) Quantification of neuritic plaques in APP23 mice with treatment starting at the age of 7 mo, the number represents mean \pm SEM. $n = 30$ mice each. *, $P < 0.0001$ by Student's t test. (E) Quantification of neuritic plaques in APP23 mice with treatment starting at the age of 9 mo, the number represents mean \pm SEM. $n = 12$ mice each. *, $P < 0.005$ by Student's t test. (F) Quantification of neuritic plaques in APP23/PS45 mice with treatment starting at the age of 6 wk, the number represents mean \pm SEM. $n = 25$ mice for control and 29 mice for VPA. *, $P < 0.0001$ by Student's t test.

mice traveled into the third quadrant, where the hidden platform was previously placed, was significantly greater with VPA treatment compared with control (9.56 ± 2.62 and 4.18 ± 1.06 ; $P < 0.005$; Fig. 2 E). These data indicate that VPA treatment significantly improves the memory deficits seen in APP23 mice. Because VPA treatment stopped a day before and there was no treatment during the behavioral testing, the effect of VPA on the behavioral performance in the mice was not just acute, but also long lasting.

Behavioral tests were also performed on the older APP23 mice administered with VPA at the age of 9 mo to assess their cognitive function. Despite a significant reduction in plaque formation, there were no significant differences in the escape

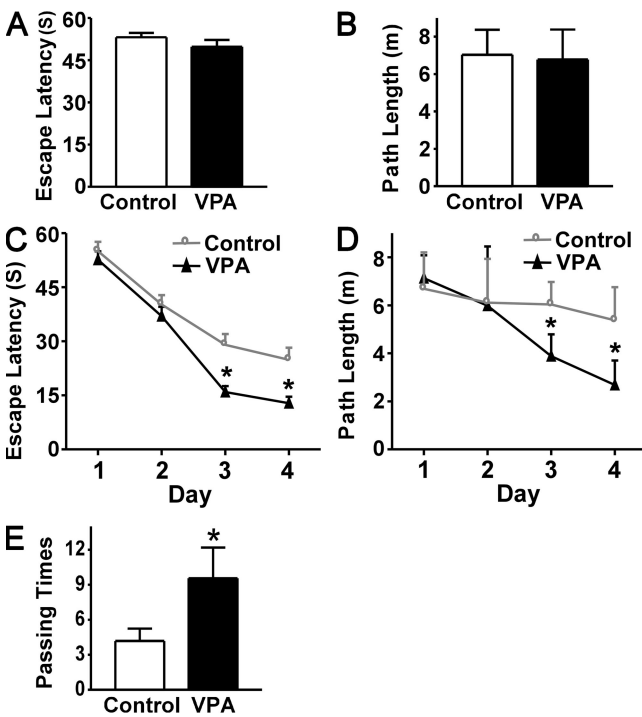


Figure 2. VPA improves memory deficits in AD transgenic mice. A Morris water maze test consists of 1 d of visible platform tests and 4 d of hidden platform tests, plus a probe trial 24 h after the last hidden platform test. Animal movement was tracked and recorded by HVS 2020 Plus image analyzer. The 7-mo APP23 age group mice were tested after 1 mo of daily VPA ($n = 30$ mice) or vehicle solution ($n = 30$ mice) injections. (A) During the first day of visible platform tests, the VPA-treated and control APP23 mice exhibited a similar latency to escape onto the visible platform. $P > 0.05$ by Student's t test. (B) The VPA-treated and control APP23 mice had similar swimming distances before escaping onto the visible platform in the visible platform test. $P > 0.05$ by Student's t test. (C) In hidden platform tests, mice were trained with 6 trials per day for 4 d. VPA-treated APP23 mice showed a shorter latency to escape onto the hidden platform on the third and fourth day. $P < 0.001$ by ANOVA. (D) The VPA-treated APP23 mice had a shorter swimming length before escaping onto the hidden platform on the third and fourth day. $P < 0.01$ by ANOVA. (E) In the probe trial on the sixth day, the VPA-treated APP23 mice traveled into the third quadrant, where the hidden platform was previously placed, significantly more times than controls. $*$, $P < 0.005$ by Student's t test.

latency and path length in the hidden platform trial of the Morris water maze test between the treatment and control groups ($P > 0.05$). Although VPA treatment only slightly improved performance in the hidden platform tests in the APP23/PS45 double-transgenic mice, VPA treatment significantly improved performance in the probe trial (7.13 ± 0.70 and 3.43 ± 1.13 ; $P < 0.05$).

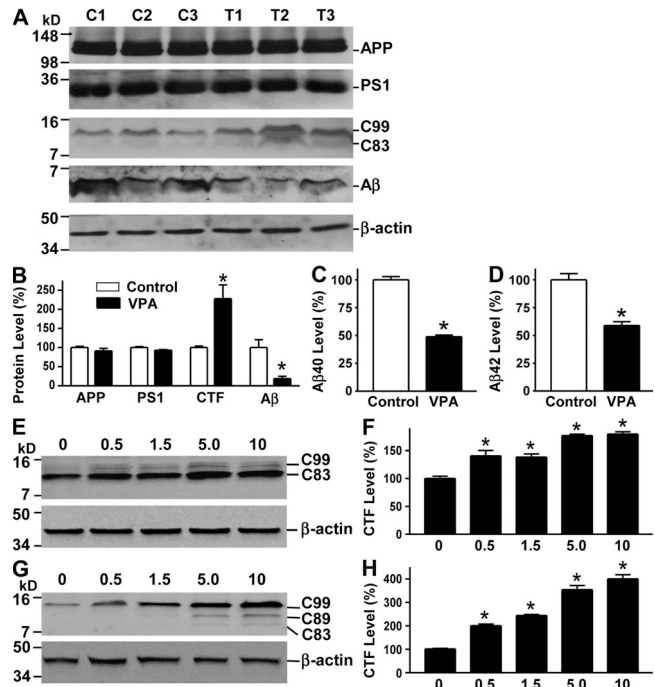


Figure 3. VPA inhibits γ -secretase cleavage of APP and A β production. (A) Half brains from VPA-treated and control APP23 mice of the 7-mo age group were lysed in RIPA-Doc lysis buffer and separated with 16% Tris-Tricine SDS-PAGE. APP full-length and CTFs (C99 and C83) were detected by C20 polyclonal antibody. PS1 was detected by anti-PS1 N-terminal antibody 231. Total A β was isolated from the brain tissues with 4G8 monoclonal antibody and detected using 6E10 anti-A β monoclonal antibody. β -Actin was detected by anti- β -actin antibody AC-15 as the internal control. (B) Quantification showed that CTFs were significantly increased, whereas A β levels were markedly reduced in VPA-treated mice. $n = 30$ each for control and VPA group. $*$, $P < 0.05$ by Student's t test. (C) ELISA assay was performed to measure A β 40 (C) and A β 42 (D) levels in the conditioned media of primary neuronal cultures derived from the brain tissues of newborn APP23/PS45 mice. The cells were cultured for a week before VPA treatment for 24 h. $n = 3$. $*$, $P < 0.005$ by Student's t test. (E) Swedish mutant APP stable cell line 20E2 was cultured and treated with different doses of VPA for 24 h, and cell lysates were subjected to Western blot analysis. C99 and C83 were detected with C20 antibody. β -Actin was detected by anti- β -actin antibody AC-15 as the internal control. (F) Quantification of CTF (C99 and C83) generation in 20E2 cells. VPA treatment significantly increased APP CTF production. $n = 4$. $*$, $P < 0.001$ by ANOVA. (G) APP C99 stable cell line H99C1 was treated with different doses of VPA for 24 h, and the CTFs (C99, C89, and C83) were detected by 9E10 antibody. β -Actin was detected by anti- β -actin antibody AC-15 as the internal control. (H) Quantification of CTFs (C99, C89, and C83) levels in H99C1 cells. VPA treatment significantly increased APP CTF production. $n = 4$. $*$, $P < 0.001$ by ANOVA.

VPA alters APP processing and inhibits A β production in vivo and in vitro

Our data clearly demonstrated that VPA treatment inhibited neuritic plaque formation and improved the memory deficits in the AD model mice. To investigate the underlying mechanism, we examined the effect of VPA on APP processing. The level of APP C-terminal fragments (CTFs) and A β in the mouse brain tissues was assayed by Western blot analysis (Fig. 3 A). VPA treatment significantly increased the levels of APP CTFs. The levels of β -secretase-generated C99 and α -secretase-generated C83 fragments were increased by $227.7 \pm 36.8\%$ in the brains of VPA-treated mice relative to controls ($P < 0.05$; Fig. 3 B). Furthermore, the production of A β was significantly inhibited by VPA, and the total A β level was decreased to $18.71 \pm 6.24\%$ in the brains of VPA-treated mice relative to controls ($P < 0.05$; Fig. 3 B). The A β ELISA assay was also performed to measure A β_{40} and A β_{42} levels in the transgenic brain tissues. The levels of A β_{40} and A β_{42} were reduced to 67.64 ± 2.89 and $34.53 \pm 1.53\%$ in VPA-treated mice relative to controls, respectively ($P < 0.05$). To further confirm VPA's effect on A β production, we measured A β_{40} and A β_{42} levels in the conditioned media of cultured primary cortical and hippocampal neurons derived from neonatal APP23/PS45 double-transgenic mice. VPA markedly reduced A β generation, decreasing A β_{40} and A β_{42} levels to 48.86 ± 1.52 and $58.90 \pm 3.43\%$, respectively, relative to controls ($P < 0.005$; Fig. 3, C and D). VPA treatment had no significant effect on APP and PS1 protein levels (Fig. 3, A and B). The increased C99 and C83 levels, together with the decreased A β production in the brains of the VPA-treated transgenic mice, indicate that VPA inhibits γ -secretase cleavage of APP proteins.

To examine the effect of VPA on APP processing in vitro, 20E2 and H99C1 cells were treated with VPA. Consistent with in vivo data from transgenic mouse models, VPA significantly increased APP C99 and C83 generation in 20E2 cells, which are a HEK293 stable cell line overexpressing the Swedish mutant APP (Fig. 3 E) (34), and the levels of total CTFs were increased by 140.58 ± 5.5 , 138.3 ± 5.58 , 176.7 ± 2.73 , and $179.64 \pm 4.10\%$ with 0.5, 1.5, 5, and 10 mM of VPA treatment, respectively ($P < 0.001$; Fig. 3 F). To further confirm the inhibitory effect of VPA on γ -secretase cleavage of APP, H99C1 cell line was established to stably overexpress APP C99, a major β -secretase cleavage product of APP (Fig. S3, available at <http://www.jem.org/cgi/content/full/jem.20081588/DC1>). VPA treatment significantly increased the levels of APP CTFs, including C99, C89, and C83 (Fig. 3 G). The levels of total CTFs were increased by 200.59 ± 4.10 , 244.09 ± 3.87 , 354.36 ± 17.30 , and $400.24 \pm 17.63\%$ with 0.5, 1.5, 5, and 10 mM of VPA treatment, respectively ($P < 0.001$; Fig. 3 H). These data clearly indicated that VPA inhibited γ -secretase processing of APP C99 protein.

VPA inhibits GSK-3 activity

Our data demonstrated that VPA significantly decreased A β production and neuritic plaque formation in AD transgenic

mice, likely by regulating APP processing through inhibition of γ -secretase activity. To further investigate the underlying mechanism of VPA's effect, we first examined its effect on APP, BACE1, and PS1 gene expression. Our data show that VPA treatment did not change the mRNA levels of these genes (Fig. 4, A–C). Previous studies suggested that GSK-3 β regulated A β formation (35–37). GSK-3 β activity is regulated by its phosphorylation at the serine 9 (S⁹) and tyrosine 216 sites (Y²¹⁶). The S⁹ phosphorylation (pGSK-3 β ^{S9}) inhibits GSK-3 β activity, whereas the Y²¹⁶ phosphorylation (pGSK-3 β ^{Y216})

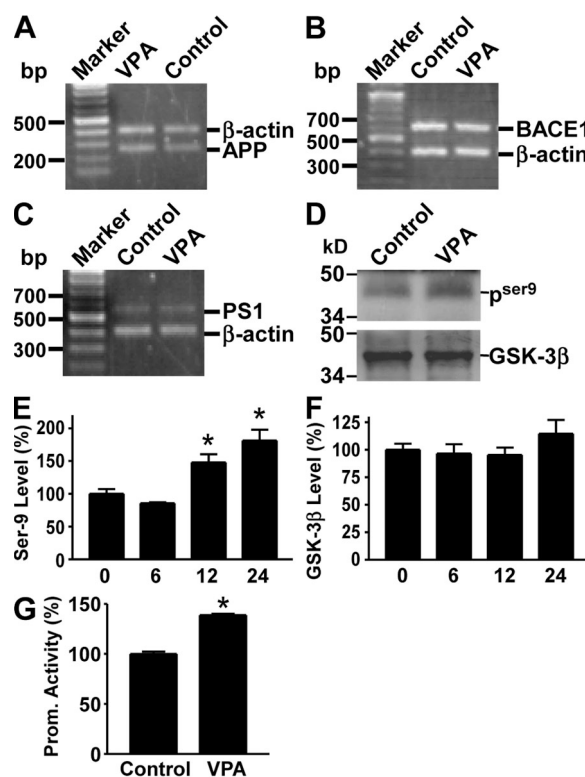


Figure 4. VPA inhibits GSK-3 β activity. Total RNA was isolated from N2a cells by TRI-Reagent (Sigma-Aldrich). A set of gene-specific primers were used to amplify APP (A), BACE1 (B), and PS1 (C) genes. β -Actin was used as an internal control. There was no difference in endogenous APP, PS1, or BACE1 mRNA levels between VPA-treated cells and controls. (D) Brain tissues from APP23/PS45 double-transgenic mice were subjected to Western blot analysis to determine the levels of total GSK-3 β and phospho-GSK-3 β ^{S9}. VPA increases phospho-GSK-3 β ^{S9} (P^{Ser9}) levels, but not total GSK-3 β levels in the transgenic mice. (E) N2a cells were treated with 5 mM of VPA for 0, 6, 12, and 24 h and lysed in RIPA-Doc buffer containing a series of serine and tyrosine phosphatase inhibitors. The cell lysates were subjected to Western blot analysis using a rabbit anti-phospho-GSK-3 β ^{Ser9} antibody. Kodak Image Analysis software was used to quantify protein level. $n = 3$. * $P < 0.001$ by ANOVA. (F) Total GSK-3 β level was also measured. (G) Promoter assay. pTOPFLASH plasmid was cotransfected with pcDNA3- β -catenin and pcDNA3-Tcf expression plasmids into N2a cells. pCMV-Rluc was also cotransfected to normalize transfection efficiency. Luciferase assay was performed 48 h after transfection. Promoter activity was indicated by the luciferase activity. VPA increased β -catenin-Tcf mediated transcription activation. $n = 4$. * $P < 0.005$ by Student's t test.

up-regulates GSK-3 β activity. To examine whether GSK-3 β mediated VPA's effect on APP processing in AD transgenic model mice, brain tissues of the double-transgenic mice were subjected to Western blot analysis for total GSK-3 β and phospho-GSK-3 β levels. We found no differences in total GSK-3 β protein levels between the VPA treatment and control mice groups; however, VPA treatment also significantly increased GSK-3 β ^{S9} levels in vivo (Fig. 4 D). Consistent with the transgenic mouse data, VPA treatment in vitro also significantly facilitated the phosphorylation of GSK-3 β at the S9 site. The level of phospho-GSK-3 β ^{S9} in VPA-treated N2a cells was increased to 147.87 ± 12.38 and $181.18 \pm 16.55\%$ after 12- and 24-h treatment ($P < 0.001$; Fig. 4 E), whereas VPA had little effect on total GSK-3 β level in N2a cells ($P > 0.05$; Fig. 4 F). Further phosphorylation screening by the Kinetworks 1.3 KPSS Phospho-site Profiling revealed that pGSK-3 β ^{Y216} levels were markedly reduced by 37%. Collectively, these data suggest that VPA negatively regulates GSK-3 β activity. To examine the effect of VPA on GSK-3 β -mediated biological function, we performed a β -catenin-Tcf reporter gene assay. Phosphorylated β -catenin by GSK-3 is rapidly degraded by the ubiquitin proteasome pathway, therefore inhibition of GSK-3 stabilizes β -catenin and activates downstream gene transcription. TOPFLASH, containing three copies of the optimal Tcf motif CCTTTGATC upstream of a minimal *c-Fos* promoter driving luciferase expression (38), were co-transfected with β -catenin and Tcf expression plasmids into N2a cells. VPA treatment significantly potentiated β -catenin-mediated transcriptional activation, resulting in higher promoter activity ($138.80 \pm 1.37\%$; $P < 0.005$; Fig. 4 G). The up-regulatory effect of VPA was abolished when the cells were transfected with mutant β -catenin cDNA. Collectively, our data indicate that regulation of APP processing and neuritic plaque formation by VPA may be mediated by its effect on the GSK-3 β signaling pathway.

DISCUSSION

There has been no effective method for the treatment or prevention of AD. Inhibition of HDAC activity with pharmacological agents demonstrated limited levels of synaptogenesis and improved learning and memory (32). Preclinical studies suggested that inhibition of A β production by altering APP processing at the β - or γ -secretase site by lithium or nonsteroidal antiinflammatory drugs could potentially be avenues for AD drug development (30, 39, 40). Here, we show that VPA, an antiepileptic drug, can serve as a highly effective anti-amyloid treatment in AD transgenic model mice. VPA can inhibit GSK-3 β , resulting in increased β -catenin protein levels (41, 42). GSK-3 β is a key component of the Wnt signaling pathway, controlling β -catenin levels and transcriptional responses required for development and cell growth. Consistent with previous reports, we found that VPA inhibited GSK-3 β activity by altering its phosphorylation state. VPA was also found to inhibit HDAC activity (29), which could improve learning and memory (32). Previous reports showed that VPA treatment not only induced synapsin I clustering in

developing axons but also increased axonal branching and formation of curved axons (43). We show that VPA not only inhibits neuritic plaque formation but also promotes neurite outgrowth in the transgenic mice.

There have been VPA clinical trials conducted on AD patients. Profenno et al. reported that doses of $<1,000$ mg/d of divalproex sodium could be tolerated by patients in a Safety and Tolerability trial of 20 outpatients with probable AD (44). In a clinical trial conducted on 14 moderate to severe institutionalized AD patients with a mean age of 85.6 yr that assessed VPA's effect on agitation and aggression, VPA treatment was found to be ineffective for the management of agitation and aggression (45). These reports had little data that addressed VPA's effect on AD pathogenesis, neuropathology, and cognitive impairments. Consistent with a previous work which showed that both lithium and VPA inhibited A β production in a Swedish mutant APP751 stable cell line and PDAPP (APPV717F) transgenic mice (37), we systematically demonstrated that in two different transgenic AD mouse models, VPA has significant beneficial effects on AD pathogenesis. VPA reduced γ -secretase cleavage of APP and A β production in vitro and in vivo, resulting in the prevention of AD-associated pathological outcomes. Furthermore, our data showed that early administration of VPA not only reduced neuritic plaque formation, but also rescued some memory deficits in AD transgenic mice. Meanwhile, we found that the inhibitory effect of VPA on neuritic plaque formation was present up to 2 mo after discontinuing administration of VPA, indicating VPA's long lasting anti-amyloid treatment potential for AD patients. However, when mice were treated with VPA at a later stage, when there was profound neuritic plaque formation, VPA could still reduce further neuritic plaque formation, albeit a lesser effect on improving memory deficits in the older mice. Our preclinical animal study indicated that VPA can have effects on neuropathology changes at early and late stages, but cognitive impairments can only be improved at an early stage intervention. These data suggest that VPA treatment should be applied at early stages of AD pathogenesis for effective improvement of pathological and cognitive impairments. This information may also provide insights for VPA clinical trial designs. Our animal study suggests that the VPA trial might not show beneficial results on late or severe AD patients, whereas it might show significant improvements in early or mild AD patients.

MATERIALS AND METHODS

Transgenic mice and VPA treatment. Animal experiment protocols were approved by The University of British Columbia Animal Care and Use committee. APP23 transgenic mice carry human APP751 cDNA with the Swedish double mutation at positions 670/671 (KM \rightarrow NL) under control of the murine Thy-1.2 expression cassette (33). PS45 transgenic mice carry human presenilin-1 cDNA with the M146V mutation. The genotype of the mice was confirmed by PCR using DNA from tail tissues. Mice were injected with 30 mg/kg VPA i.p. at the same time each day. Control mice were injected with PBS as a vehicle. We tabulated daily food and water consumption for each mouse.

Morris water maze. The water maze test was performed in a 1.5-m-diam pool. A 10-cm-diam platform was placed in the southeastern quadrant in the hidden trials. The procedure consisted of 1 d of visible platform tests and 4 d of hidden platform tests, plus a probe trial 24 h after the last hidden platform test. In the visible platform test, mice were tested for 5 contiguous trials, with an intertrial interval of 30 min. In the hidden platform tests, mice were trained for 6 trials, with an intertrial interval of 1 h. Tracking of animal movement was achieved with an HVS 2020 Plus image analyzer (HVS Image). The data were analyzed by two-way ANOVA.

Immunohistochemical staining. Mice were killed after behavioral testing, and one half of the brains were immediately homogenized for protein, RNA, or DNA extraction. The other half of the brains were fixed in freshly depolymerized 4% paraformaldehyde and sectioned with a Cryostat (Leica) to 30 μ m thickness. Every sixth slice with the same reference position was mounted onto slides for staining. Immunocytochemical staining was performed on floating sections. The slices were immunostained with biotinylated monoclonal 4G8 antibody (Signet Laboratories) in 1:500 dilution. Plaques were visualized by the ABC and DAB method and counted under microscopy at 40 \times magnification. Plaques were quantitated, and the mean plaque count per slice was recorded for each mouse. The data were analyzed by two-way ANOVA. Thioflavin S staining of plaques was performed with 1% thioflavin S, and the green fluorescence-stained plaques were visualized using fluorescence microscopy. For MAP-2 staining, sections were immunostained with anti-MAP-2 (Signet Laboratories).

Cell culture, transfection, and luciferase assay. All cells were maintained at 37°C in an incubator containing 5% CO₂. The 20E2 cell line is a Swedish mutant APP stable HEK cell line. Cells were transfected with plasmid DNA using Lipofectamine 2000 (Invitrogen). HEK293 cells were stably transfected with pZ-C99mycHis to generate the H99C1 cell line. H99C1 cells stably overexpress APP C99, a major β -secretase product of APP. The mycHis-tagged C99 protein in H99C1 cells can be detected by both anti-myc 9E10 antibody and anti-APP C-terminal antibody C20. For primary neuronal cultures, hippocampal and neocortical tissues were removed from newborn mice at postnatal day 1, and gently digested with trypsin (0.025% EDTA; Invitrogen). The cells were suspended in neurobasal medium supplemented with B27 (Invitrogen) and plated at a density of 2×10^6 cells per 35-mm plate coated with 0.01 mg/ml poly-D-lysine (Sigma-Aldrich). Tails from the newborn mice were used to isolate genomic DNA for genotyping. The primary cultures were maintained at 37°C in a humidified incubator containing 5% CO₂. For the β -catenin-mediated transcriptional activation assay, pTOPFLASH plasmid was co-transfected with pcDNA3- β -catenin and pcDNA3-Tcf expression plasmids into N2a cells. The *Renilla* (sea pansy) luciferase vector pCMV-Rluc was cotransfected to normalize transfection efficiency. Luciferase assay was performed 48 h after transfection with Dual-Luciferase Reporter Assay system (Promega), as previously described (2).

Immunoblotting. Brain tissue or cells were lysed in RIPA lysis buffer (1% Triton X-100, 1% sodium deoxycholate, 4% SDS, 0.15 M NaCl, and 0.05 M Tris-HCl, pH 7.2) supplemented with protease inhibitors (Complete; Roche). The lysates were resolved by 12% SDS-PAGE or 16% tris-tricine PAGE. Immunoblotting was performed as previously described (6). Rabbit anti-APP C-terminal polyclonal antibody C20 was used to detect APP and its CTF products. PS1 was detected by anti-PS1 N-terminal antibody 231. A β was immunoprecipitated from 50- μ l aliquots of the tissue extract with 5 μ l of primary antibody 4G8 plus protein A/G beads. Immunoprecipitates were subjected to 16% Tris-Tricine SDS-PAGE. The level of GSK-3 β inhibition was assessed using a rabbit anti-phospho-GSK-3 β ^{S9} antibody (Cell Signaling Technology, Inc.). The level of GSK-3 β activation was assessed using a rabbit anti-phospho-GSK-3 α ^{Y279}/ β ^{Y216} antibody (BioSource International, Inc.). Total GSK-3 β was determined using a pan-specific mouse anti-GSK-3 α / β antibody (BioSource International, Inc.). Internal control β -actin was analyzed using monoclonal antibody AC-15 (Sigma-Aldrich).

RT-PCR. RNA was isolated from cells using TRI-Reagent (Sigma-Aldrich). PowerScript reverse transcription (Invitrogen) was used to synthesize the first-strand cDNA from an equal amount of the RNA sample following the manufacturer's instruction. The newly synthesized cDNA templates were further amplified by Platinum *Taq* DNA polymerase (Invitrogen) in a 25- μ l reaction. The following primers were used to specifically amplify APP, PS1, and BACE1 genes: BACE1, forward 5'-ACCGACGAAGAGTCG-GAGGAG-3' and reverse 5'-CACAAATGCTCTTGTGCATAG-3'; APP, forward 5'-CGGAATTCCTTGGTGTCTTTCGAGAAG-3' and reverse 5'-CGGAATTCGGTCTGCATCTCTCAAAG-3'; PS1, forward 5'-GGATCCGCCACCATGGTGTGGTGGTGAATATGGC-3' and reverse 5'-CGGGATCCCTAGATATAAAAATTGATGG-3'.

β -Actin was used as an internal control. The samples were analyzed on a 1.2% agarose gel.

Kinetwork KPSS 1.3 PhosphoSite analysis. N2A cells were treated with 5 mM of VPA for 12 h, followed by homogenizing in lysis buffer containing 0.5% Triton X-100, 2 mM EGTA, 5 mM EDTA, 20 mM MOPS, 200 mM sodium orthovanadate, 25 mM β -glycerophosphate, 20 mM sodium pyrophosphate, 30 mM sodium fluoride, 1 mM PMSF, and 1 complete mini protease inhibitor cocktail tablet (Roche Diagnostics). The samples were diluted in 4 \times SDS-sample buffer to give a final protein concentration of 1 μ g/ μ l. The samples were then boiled and sent to Kinexus Bioinformatics Corp. for the Kinetworks KPSS 1.3 Phospho-Site multiimmunoblotting analyses. The KPSS 1.3 screen tracks the phosphorylation levels of >35 protein kinases and their substrates.

A β 40/42 ELISA assay. Tissue extracts from transgenic mouse hippocampal and neocortical regions and conditioned cell culture media were collected. Protein inhibitors and AEBSF were added to prevent degradation of A β peptides. The concentration of A β 40/42 was detected by β -amyloid 1-40 or 1-42 Colorimetric ELISA kit (BioSource International, Inc.) according to the manufacturer's instructions.

Online supplemental material. Fig. S1 shows the genotyping of the AD transgenic mice. Fig. S2 shows the results of VPA's effect on plaque formation in different age groups of APP23 mice. Fig. S3 shows the generation of human APP C99 stable cell line H99C1. Online supplemental material is available at <http://www.jem.org/cgi/content/full/jem.20081588/DC1>.

We thank Michelle A. Christensen and Clement Kwok for their technical assistance. We also thank Kelley Bromley-Brits for helpful discussion.

This work was supported by the Canadian Institutes of Health Research (CIHR), Jack Brown and Family Alzheimer's Research Foundation, and the Michael Smith Foundation for Health Research (MSFHR; to W. Song). W. Song is the holder of the Canada Research Chair in Alzheimer's Disease. H. Qing, S. Wei, and W. Zhou were recipients of the Arthur and June Willms Fellowships. G. He was supported by the China Scholarship Council award. P.T. Ly is supported by a MSFHR Senior Graduate Studentship. C. J. Fox was supported by a CIHR Doctoral Research Award and a MSFHR Senior Graduate Studentship.

The authors have no conflicting financial interests.

Submitted: 21 July 2008

Accepted: 1 October 2008

REFERENCES

- Glenner, G.G., and C.W. Wong. 1984. Alzheimer's disease: initial report of the purification and characterization of a novel cerebrovascular amyloid protein. *Biochem. Biophys. Res. Commun.* 120:885-890.
- Sun, X., Y. Wang, H. Qing, M.A. Christensen, Y. Liu, W. Zhou, Y. Tong, C. Xiao, Y. Huang, S. Zhang, et al. 2005. Distinct transcriptional regulation and function of the human BACE2 and BACE1 genes. *FASEB J.* 19:739-749.
- Roberds, S.L., J. Anderson, G. Basi, M.J. Bienkowski, D.G. Branstetter, K.S. Chen, S.B. Freedman, N.L. Frigon, D. Games, K. Hu, et al. 2001. BACE knockout mice are healthy despite lacking the primary beta-secretase

- activity in brain: implications for Alzheimer's disease therapeutics. *Hum. Mol. Genet.* 10:1317–1324.
4. Luo, Y., B. Bolon, S. Kahn, B.D. Bennett, S. Babu-Khan, P. Denis, W. Fan, H. Kha, J. Zhang, Y. Gong, et al. 2001. Mice deficient in BACE1, the Alzheimer's beta-secretase, have normal phenotype and abolished beta-amyloid generation. *Nat. Neurosci.* 4:231–232.
 5. Cai, H., Y. Wang, D. McCarthy, H. Wen, D.R. Borchelt, D.L. Price, and P.C. Wong. 2001. BACE1 is the major beta-secretase for generation of Abeta peptides by neurons. *Nat. Neurosci.* 4:233–234.
 6. Sun, X., G. He, and W. Song. 2006. BACE2, as a novel APP theta-secretase, is not responsible for the pathogenesis of Alzheimer's disease in Down syndrome. *FASEB J.* 20:1369–1376.
 7. Takasugi, N., T. Tomita, I. Hayashi, M. Tsuruoka, M. Niimura, Y. Takahashi, G. Thinakaran, and T. Iwatsubo. 2003. The role of presenilin cofactors in the gamma-secretase complex. *Nature.* 422:438–441.
 8. De Strooper, B., W. Annaert, P. Cupers, P. Saftig, K. Craessaerts, J.S. Mumm, E.H. Schroeter, V. Schrijvers, M.S. Wolfe, W.J. Ray, et al. 1999. A presenilin-1-dependent gamma-secretase-like protease mediates release of Notch intracellular domain. *Nature.* 398:518–522.
 9. De Strooper, B., P. Saftig, K. Craessaerts, H. Vanderstichele, G. Guhde, W. Annaert, K. Von Figura, and F. Van Leuven. 1998. Deficiency of presenilin-1 inhibits the normal cleavage of amyloid precursor protein. *Nature.* 391:387–390.
 10. Song, W., P. Nadeau, M. Yuan, X. Yang, J. Shen, and B.A. Yankner. 1999. Proteolytic release and nuclear translocation of Notch-1 are induced by presenilin-1 and impaired by pathogenic presenilin-1 mutations. *Proc. Natl. Acad. Sci. USA.* 96:6959–6963.
 11. Zhang, Z., P. Nadeau, W. Song, D. Donoviel, M. Yuan, A. Bernstein, and B.A. Yankner. 2000. Presenilins are required for gamma-secretase cleavage of beta-APP and transmembrane cleavage of Notch-1. *Nat. Cell Biol.* 2:463–465.
 12. Zhou, S., H. Zhou, P.J. Walian, and B.K. Jap. 2005. CD147 is a regulatory subunit of the gamma-secretase complex in Alzheimer's disease amyloid beta-peptide production. *Proc. Natl. Acad. Sci. USA.* 102:7499–7504.
 13. Chen, F., H. Hasegawa, G. Schmitt-Ulms, T. Kawarai, C. Bohm, T. Katayama, Y. Gu, N. Sanjo, M. Glista, E. Rogava, et al. 2006. TMP21 is a presenilin complex component that modulates gamma-secretase but not epsilon-secretase activity. *Nature.* 440:1208–1212.
 14. Wolfe, M.S., W. Xia, B.L. Ostaszewski, T.S. Diehl, W.T. Kimberly, and D.J. Selkoe. 1999. Two transmembrane aspartates in presenilin-1 required for presenilin endoproteolysis and gamma-secretase activity. *Nature.* 398:513–517.
 15. Li, Y.M., M. Xu, M.T. Lai, Q. Huang, J.L. Castro, J. DiMuzio-Mower, T. Harrison, C. Lellis, A. Nadin, J.G. Neduvilil, et al. 2000. Photoactivated gamma-secretase inhibitors directed to the active site covalently label presenilin 1. *Nature.* 405:689–694.
 16. Ikeuchi, T., and S.S. Sisodia. 2003. The Notch ligands, Delta1 and Jagged2, are substrates for presenilin-dependent "gamma-secretase" cleavage. *J. Biol. Chem.* 278:7751–7754.
 17. LaVoie, M.J., and D.J. Selkoe. 2003. The Notch ligands, Jagged and Delta, are sequentially processed by alpha-secretase and presenilin/gamma-secretase and release signaling fragments. *J. Biol. Chem.* 278:34427–34437.
 18. Six, E., D. Ndiaye, Y. Laabi, C. Brou, N. Gupta-Rossi, A. Israel, and F. Logeat. 2003. The Notch ligand Delta1 is sequentially cleaved by an ADAM protease and gamma-secretase. *Proc. Natl. Acad. Sci. USA.* 100:7638–7643.
 19. Ni, C.Y., M.P. Murphy, T.E. Golde, and G. Carpenter. 2001. gamma-Secretase cleavage and nuclear localization of ErbB-4 receptor tyrosine kinase. *Science.* 294:2179–2181.
 20. Marambaud, P., P.H. Wen, A. Dutt, J. Shioi, A. Takashima, R. Siman, and N.K. Robakis. 2003. A CBP binding transcriptional repressor produced by the PS1/epsilon-cleavage of N-cadherin is inhibited by PS1 FAD mutations. *Cell.* 114:635–645.
 21. Kim, D.Y., L.A. Ingano, and D.M. Kovacs. 2002. Nectin-1alpha, an immunoglobulin-like receptor involved in the formation of synapses, is a substrate for presenilin/gamma-secretase-like cleavage. *J. Biol. Chem.* 277:49976–49981.
 22. May, P., Y.K. Reddy, and J. Herz. 2002. Proteolytic processing of low density lipoprotein receptor-related protein mediates regulated release of its intracellular domain. *J. Biol. Chem.* 277:18736–18743.
 23. Sherrington, R., E.I. Rogava, Y. Liang, E.A. Rogava, G. Levesque, M. Ikeda, H. Chi, C. Lin, G. Li, K. Holman, et al. 1995. Cloning of a gene bearing missense mutations in early-onset familial Alzheimer's disease. *Nature.* 375:754–760.
 24. Levy-Lahad, E., W. Wasco, P. Poorkaj, D.M. Romano, J. Oshima, W.H. Pettingell, C.E. Yu, P.D. Jondro, S.D. Schmidt, K. Wang, et al. 1995. Candidate gene for the chromosome 1 familial Alzheimer's disease locus. *Science.* 269:973–977.
 25. Rogava, E.I., R. Sherrington, E.A. Rogava, G. Levesque, M. Ikeda, Y. Liang, H. Chi, C. Lin, K. Holman, T. Tsuda, et al. 1995. Familial Alzheimer's disease in kindreds with missense mutations in a gene on chromosome 1 related to the Alzheimer's disease type 3 gene. *Nature.* 376:775–778.
 26. Perucca, E. 2002. Pharmacological and therapeutic properties of valproate: a summary after 35 years of clinical experience. *CNS Drugs.* 16:695–714.
 27. Czuczwar, S.J., and P.N. Patsalos. 2001. The new generation of GABA enhancers. Potential in the treatment of epilepsy. *CNS Drugs.* 15:339–350.
 28. Yuan, P.X., L.D. Huang, Y.M. Jiang, J.S. Gutkind, H.K. Manji, and G. Chen. 2001. The mood stabilizer valproic acid activates mitogen-activated protein kinases and promotes neurite growth. *J. Biol. Chem.* 276:31674–31683.
 29. Williams, R.S., L. Cheng, A.W. Mudge, and A.J. Harwood. 2002. A common mechanism of action for three mood-stabilizing drugs. *Nature.* 417:292–295.
 30. Phiel, C.J., C.A. Wilson, V.M. Lee, and P.S. Klein. 2003. GSK-3alpha regulates production of Alzheimer's disease amyloid-beta peptides. *Nature.* 423:435–439.
 31. Harwood, A.J. 2003. Neurodevelopment and mood stabilizers. *Curr. Mol. Med.* 3:472–482.
 32. Fischer, A., F. Sananbenesi, X. Wang, M. Dobbin, and L.-H. Tsai. 2007. Recovery of learning and memory is associated with chromatin remodelling. *Nature.* 447:178–182.
 33. Sun, X., G. He, H. Qing, W. Zhou, F. Dobie, F. Cai, M. Staufenbiel, L.E. Huang, and W. Song. 2006. Hypoxia facilitates Alzheimer's disease pathogenesis by up-regulating BACE1 gene expression. *Proc. Natl. Acad. Sci. USA.* 103:18727–18732.
 34. Qing, H., W. Zhou, M.A. Christensen, X. Sun, Y. Tong, and W. Song. 2004. Degradation of BACE by the ubiquitin-proteasome pathway. *FASEB J.* 18:1571–1573.
 35. Eickholt, B.J., G.J. Towers, W.J. Ryves, D. Eikel, K. Adley, L.M. Ylisen, N.H. Chadborn, A.J. Harwood, H. Nau, and R.S. Williams. 2005. Effects of valproic acid derivatives on inositol trisphosphate depletion, teratogenicity, glycogen synthase kinase-3beta inhibition, and viral replication: a screening approach for new bipolar disorder drugs derived from the valproic acid core structure. *Mol. Pharmacol.* 67:1426–1433.
 36. Ryan, K.A., and S.W. Pimplikar. 2005. Activation of GSK-3 and phosphorylation of CRMP2 in transgenic mice expressing APP intracellular domain. *J. Cell Biol.* 171:327–335.
 37. Su, Y., J. Ryder, B. Li, X. Wu, N. Fox, P. Solenberg, K. Brune, S. Paul, Y. Zhou, F. Liu, and B. Ni. 2004. Lithium, a common drug for bipolar disorder treatment, regulates amyloid-beta precursor protein processing. *Biochemistry.* 43:6899–6908.
 38. Korinek, V., N. Barker, P.J. Morin, D. van Wichen, R. de Weger, K.W. Kinzler, B. Vogelstein, and H. Clevers. 1997. Constitutive transcriptional activation by a beta-catenin-Tcf complex in APC-/- colon carcinoma. *Science.* 275:1784–1787.
 39. Weggen, S., J.L. Eriksen, P. Das, S.A. Sagi, R. Wang, C.U. Pietrzik, K.A. Findlay, T.E. Smith, M.P. Murphy, T. Bulter, et al. 2001. A subset of NSAIDs lower amyloidogenic Abeta42 independently of cyclooxygenase activity. *Nature.* 414:212–216.
 40. Li, Y., W. Zhou, Y. Tong, G. He, and W. Song. 2006. Control of APP processing and Abeta generation level by BACE1 enzymatic activity and transcription. *FASEB J.* 20:285–292.

41. Kim, A.J., Y. Shi, R.C. Austin, and G.H. Werstuck. 2005. Valproate protects cells from ER stress-induced lipid accumulation and apoptosis by inhibiting glycogen synthase kinase-3. *J. Cell Sci.* 118:89–99.
42. Chen, G., L.D. Huang, Y.M. Jiang, and H.K. Manji. 1999. The mood-stabilizing agent valproate inhibits the activity of glycogen synthase kinase-3. *J. Neurochem.* 72:1327–1330.
43. Hall, A.C., A. Brennan, R.G. Goold, K. Cleverley, F.R. Lucas, P.R. Gordon-Weeks, and P.C. Salinas. 2002. Valproate regulates GSK-3-mediated axonal remodeling and synapsin I clustering in developing neurons. *Mol. Cell. Neurosci.* 20:257–270.
44. Profenno, L.A., L. Jakimovich, C.J. Holt, A. Porsteinsson, and P.N. Tariot. 2005. A randomized, double-blind, placebo-controlled pilot trial of safety and tolerability of two doses of divalproex sodium in outpatients with probable Alzheimer's disease. *Curr. Alzheimer Res.* 2:553–558.
45. Herrmann, N., K.L. Lanctot, L.S. Rothenburg, and G. Eryavec. 2007. A placebo-controlled trial of valproate for agitation and aggression in Alzheimer's disease. *Dement. Geriatr. Cogn. Disord.* 23:116–119.